

A Novel Coupling Method of Power Supplies With High Power Density, Efficiency, and Fast Dynamic Response for Spacecraft Hollow Cathode Power Supply Applications

Ming Fu, *Student Member, IEEE*, Donglai Zhang, *Member, IEEE*, and Tiejai Li

Abstract—This paper presents a coupling method of power supplies to improve power density, efficiency, and dynamic response by taking the case of heater supply, ignitor supply, and keeper supply for hollow cathode of an all electric propulsion (AEP) Hall thruster. The working principle and timing characteristic of the coupled supply, as well as the three-loop control, current sampling and chopping switch control are also illustrated. With the proposed coupling method, the power density is improved since three supplies are coupled into one supply. Additionally, the test on the coupled supply prototype with 200 W maximum output power shows that the efficiency of the coupled supply could reach up to 89.7%, increasing by 3.9%–14.2% as being compared with that of traditional three supplies with heater current between 4 and 10 A, and the joint test of the coupled supply with an AEP hall thruster proves the achievement of fast dynamic response and the ability to extend useful life of hollow cathode. Hence, the coupling method proposed in this paper could achieve the power supply system with high power density, efficiency, and fast dynamic response.

Index Terms—Coupling, hollow cathode, power density, three-loop control.

I. INTRODUCTION

WITH the limitation on bulk, cost and specific payload characteristic, high power density, high efficiency, and fast dynamic response are of the most important consideration

Manuscript received April 5, 2016; revised July 9, 2016 and July 31, 2016; accepted September 12, 2016. Date of publication September 16, 2016; date of current version February 27, 2017. This work was supported by the Basic Research Project from State Administration of Science, Technology, and Industry for National Defence, PRC under Grant JSZL2015603B004, and by the Shenzhen Science and Technology Plan Project under Grants JSGG20150529114007828 and JCYJ20150529153003796. Recommended for publication by Associate Editor R. Burgos.

M. Fu is with the Power Electronic and Motion Control Research Center, Harbin Institute of Technology Shenzhen Graduate School, Shenzhen 518055, China, and also with the Shenzhen Academy of Aerospace Technology, Shenzhen 518057, China (e-mail: fm701.student@sina.com).

D. Zhang is with the Power Electronic and Motion Control Research Center, Harbin Institute of Technology Shenzhen Graduate School, Shenzhen 518055, China (e-mail: zhangdl@hitsz.edu.cn).

T. Li is with the School of Electrical Engineering and Automation, Harbin Institute of Technology, Harbin 150001, China, and also with the Shenzhen Academy of Aerospace Technology, Shenzhen 518057, China (e-mail: litc611@public.hr.hl.cn).

Color versions of one or more of the figures in this paper are available online at <http://ieeexplore.ieee.org>.

Digital Object Identifier 10.1109/TPEL.2016.2610442

during the design of power supplies for aerospace or specific industrial equipment [1]–[5]. For single supply, the achievement of aforementioned characteristics has been widely investigated by increasing switching frequency through employment of new switching devices (such as Silicon Carbide (SiC) and Gallium Nitride (GaN) transistors) or series-parallel connection of switching devices [2], [5]–[7], or investigated by employing novel topology of power converter [8], [9], ripple cancellation technology [10], [11], filtering inductance coupling technology [1], [12]–[14] or advanced control technique [4], [12], [15]. For multiple supplies, a common method in the industry to increase the power density is to use the multipleoutput isolated converter, for which, each output voltage is always constant, and the investigation mainly focuses on how to ensure low output voltage regulation and how to eliminate the interaction and cross-regulation between different outputs when there is change in payload power or input voltage, or there is mismatching between output payload power of each channel, etc [16]–[20]. However, the multipleoutput isolated converter is not applicable in the occasion when each output outputs changeable current/voltage for different functions and there is a certain timing between each output.

For power system of specific industrial equipment, which are often constituted of more than one supply with each supply powering the equipment in a certain sequence [2], [21]–[23], the optimal design in the aspect of power system should be considered to achieve high power density, high efficiency, and fast dynamic response. The coupling of power supplies could fit this need, and it can make one supply possess functions of one more supplies without the change of power supply functions, which is achieved through appropriate topology coupling and corresponding control design. In fact, this technique has been widely investigated to significantly improve power density, efficiency, and dynamic response of power system [14], [24], [25].

Based on the consideration that electric propulsion (EP) has increasingly become the main configuration of propulsion platform in spacecraft [26]–[28] with ion thruster and stationary plasma thruster of the most wide application [22], [23], [29], [30], as well as the importance of hollow cathode to the ionization of xenon in thruster [29], [31]–[33], a novel coupling method of power supplies was proposed by taking the case of power system for hollow cathode.

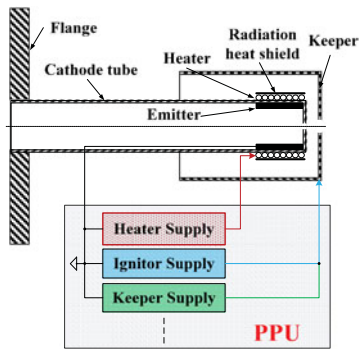


Fig. 1. Scheme of the hollow cathode and its power supplies in EP.

Fig. 1 shows the hollow cathode applied in a stationary plasma thruster and its power supplies in power processing unit (PPU) of EP. Among which, hollow cathode consists of flange, cathode tube, heater, emitter, radiation heat shield, and cathode keeper; and traditionally, in most PPU, there are often three independent supplies for hollow cathode, that is, heater supply, ignitor supply, and keeper supply, with the latter two connecting to cathode keeper and all three outputting power based on the same basis ground. Since there would be a self-heating phenomenon in hollow cathode and long-delayed regulation on the heating power after successful ignition of thruster following the successful ignition of hollow cathode [34]–[36], the above traditional power supply system for hollow cathode, which are also shown in this literatures [29], [33], possesses the following disadvantages: decreased useful life of hollow cathode due to its long duration under excessive high temperature, and large bulk and weight resulted from presence of three supplies.

In this paper, the novel coupling method was proposed based on the working timing and electrical characteristic of the above power system for hollow cathode. It should be noted that this coupling method is not limited to the application in hollow cathode power supplies, that is, it can be also applicable in other power supplies with certain working timing and different settable output voltage/current, such as power supplies for arcjet propulsion system, travelling wave tube, or some plasma devices, etc [37], [38]. The following work has been illustrated for the novel coupling method: coupling design, working principle, timing characteristic, and control strategy. Besides, the coupled supply prototype with 200 W maximum output power has been designed and tested with results showing that there is increased efficiency and dynamic response of the coupled supply as being compared with the traditional three supplies, additionally, the power density is also improved since three supplies are coupled into one supply, thus resolving the aforementioned problems, in agreement with the expected coupling design purpose.

II. COUPLING DESIGN

In this paper, the coupling is designed by taking the case of heater supply, ignitor supply, and keeper supply for the hollow cathode of an all electric propulsion (AEP) Hall thruster with specifications illustrated in Table I.

For hollow cathode, its working characteristic is shown as follows. The heating filament in heater is first heated to about

TABLE I
SPECIFICATIONS OF THE SUPPLY FOR HOLLOW CATHODE

Parameter	Value	Comments
Input voltage V_{in}	100 ± 3 V	Regulated power bus
Ignitor voltage V_{ik}	300 ± 20 V	
Ignitor pulse width	5 ms/100 ms	Settable
Keeper current limit I_{keeper}	0.3 – 1.5 A	Step of 0.1 A, rated current of 0.5 A
Keeper Voltage limit V_k	≤ 60 V	Maximum output voltage
Heater current I_h	4 – 10 A	Step of 0.1 A, rated current of 8 A
Heater Voltage limit $V_{h,max}$	≤ 20 V	Maximum clamping output voltage
Output power P_{out}	≤ 200 W	Total output power of three supplies
Efficiency η	$> 80\%$	Rated condition

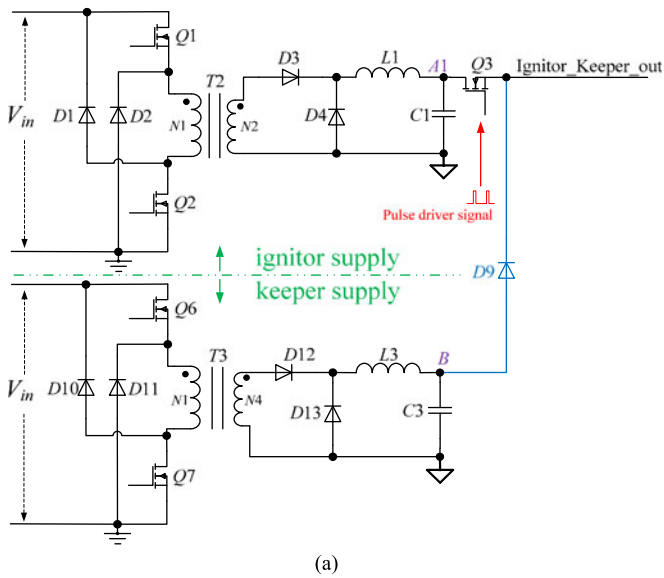
1200 °C by heater supply to make emitter generate electrons. The electrons then excite xenon to transform to plasma under the high voltage pulse provided by ignitor supply, and the successful ignition is obtained. At the moment of successful ignition, the impedance between cathode keeper and basis ground (shown below as keeper impedance) decreases sharply, leading to the quick decrease of voltage between cathode keeper and basis ground (shown below as keeper voltage). By detecting the sharp decrease of keeper voltage, ignitor supply identifies successful ignition, and then stops outputting power so as to prevent ignitor supply and cathode keeper from being damaged. At the shutdown moment of ignitor supply, keeper supply provides low-voltage constant current to maintain plasma state of xenon in hollow cathode. After successful ignition of thruster following the successful ignition of hollow cathode, there would be a self-heating phenomenon and thus increased temperature in hollow cathode. When each function part of thruster starts up and works stably, the EP control system sends commands to shut down heater supply and ignitor supply.

The coupling method of the above heater supply, ignitor supply, and keeper supply is detailed below, which is based on dual-switch forward topology.

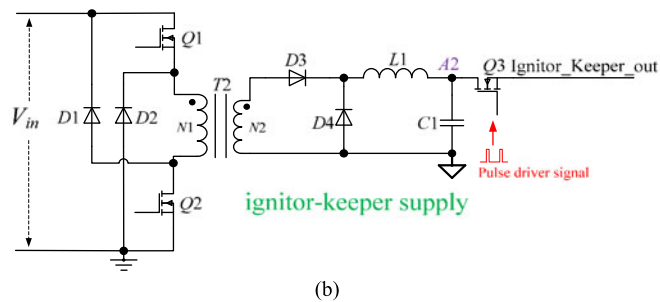
A. Coupling of Ignitor Supply and Keeper Supply Into Ignitor-keeper Supply

Based on the timing characteristic of ignitor supply and keeper supply, which is illustrated below, as well as the same input and output for these two supplies, the coupling of these two supplies into ignitor-keeper supply is considered at first. Fig. 2(a) and (b) show the topology of ignitor supply and keeper supply before coupling and after coupling, respectively.

In Fig. 2(a), for ignitor supply, the dc voltage (output voltage at point A1, V_{A1}) is constant at 300 V through closed-loop control (also called voltage PID control loop), while the high voltage pulse is generated through switch $Q3$, which works at chopping control mode with pulse width/period of 5 ms/100 ms; for keeper supply, the current through filter inductor $L3$ (also the output current of keeper supply) is constant at set value through closed-loop control (also called current PID control loop), meanwhile, the maximum output voltage at point B is limited to 60 V by setting the maximum duty cycle of pulse width modulation (PWM) for primary switches [see $Q6$, $Q7$ in Fig. 2(a)]. The Ignitor_Keeper_out, which connects to cathode



(a)

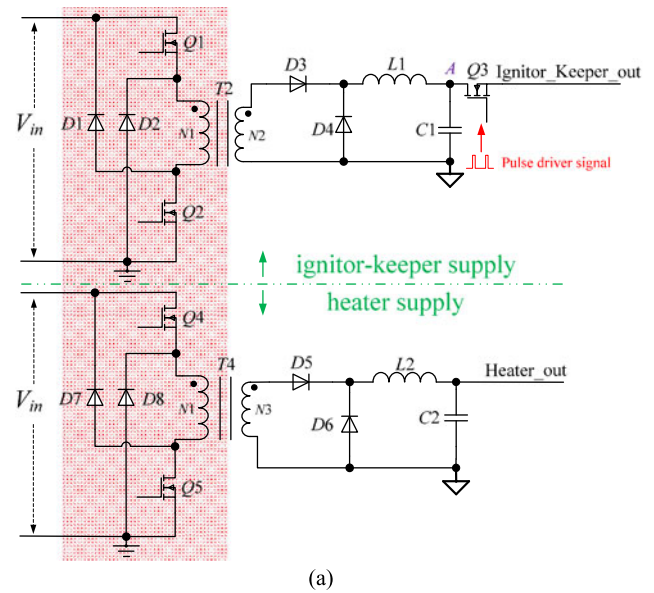


(b)

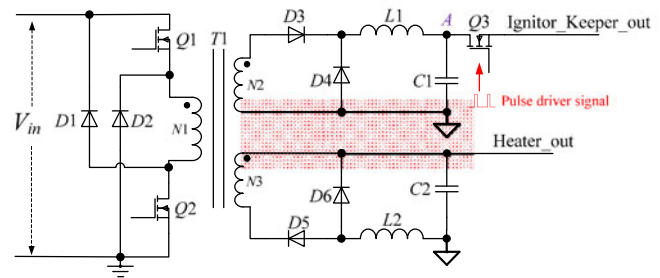
Fig. 2. Topology of ignitor supply and keeper supply: (a) before coupling; and (b) after coupling.

keeper, is formed by connecting the output of keeper supply and $Q3$ through a high voltage diode $D9$.

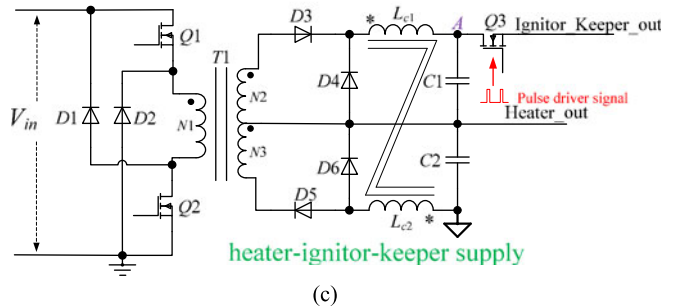
In Fig. 2(b), the topology possesses the function of igniting and keeping, and the output of ignitor supply and keeper supply is controlled through an appropriate control strategy. That is, the ignitor voltage PID control loop is formed by sampling voltage at point $A2$ (V_{A2}), and the keeper current PID control loop is formed by sampling the current through filter inductor $L1$, and the PWM duty cycle is regulated through choosing the smaller output of the above two PID control loops. Before successful ignition of hollow cathode, the keeper impedance is high, and the current through cathode keeper is 0, and the keeper current PID control loop is off work; at this time, the ignitor voltage PID control loop is on work to keep V_{A2} constant at 300 V. After successful ignition, the keeper impedance decreases sharply, then V_{A2} decreases and ignitor voltage PID control loop is off work with output error voltage at the maximum value. When V_{A2} decreases to smaller than 60% peak voltage (180 V), which is detected by the control circuit of $Q3$, the successful ignition is identified. At this moment, different from the off state of $Q3$ in Fig. 2(a), $Q3$ is set at on state all the time and keeper impedance decreases further. When the keeper impedance decreases to that the current through cathode keeper increases to the set value of keeper supply, the keeper current PID control loop starts to work to keep current through $L1$ constant at the set value.



(a)



(b)



(c)

Fig. 3. Topology of: (a) ignitor-keeper supply and heater supply before coupling; (b) ignitor-keeper supply and heater supply with coupling of dc-ac conversion in primary side; and (c) the final coupled supply: heater-ignitor-keeper supply.

B. Coupling of Heater Supply and Ignitor-Keeper Supply Into Heater-Ignitor-keeper Supply

The further coupling of ignitor-keeper supply with heater supply is shown in Fig. 3. Fig. 3(a) shows the topology of ignitor-keeper supply and heater supply before coupling, from which it can be seen that the ignitor-keeper supply and heater supply both adopt dual-switch forward topology and work at the same time, thus, the function parts of dc-ac conversion in primary side are coupled at first, which is shown in Fig. 3(b). In Fig. 3(b), except for the coupling of primary sides, there are also some changes on secondary rectifier circuit, that is, rectifier diode $D5$ and output filter inductor $L2$ in heater supply are

moved to the earth ground. Following this change, the rectifier circuit of ignitor-keeper supply is overlaid onto that of heater supply with the same ground return, and then the output filter inductor of ignitor-keeper supply (L_1) and that of heater supply (L_2) are coupled into one coupling inductor L_c by winding on one magnetic core, finally, the heater-ignitor-keeper supply obtained from the proposed coupling method possesses the topology shown in Fig. 3(c). With the above overlay operation, the voltage at Heater_out is added onto the voltage at point A (V_A), that is, the ratio of V_A to input voltage V_{in} changes to $(N_2 + N_3):N_1$ from $N_2:N_1$, thus, the turn number N_2 decreases and the design of main transformer (T_1) is simplified. Additionally, the above coupling of two inductors L_1 and L_2 can bring the following advantages: increase in the power density of supply, decrease in the output current ripple of ignitor-keeper supply, and decrease on the cross regulation of V_A during the regulation of heater supply.

Through the above coupling, three independent supplies are integrated into a heater-ignitor-keeper supply, which brings the following three advantages as being compared with the traditional three supplies [29], [33]:

- 1) The power density is significantly increased since traditional three supplies become one supply.
- 2) The dynamic response of I_h is significantly enhanced, that is, at the moment of successful ignition, the output power of heater supply decreases sharply and the current through cathode keeper is limited and constant at the set value soon. Thus, with enough protection, the hollow cathode has longer useful life.
- 3) The total efficiency increases since the power loss from auxiliary power supply, primary side switching transistors, main transformer, etc, decreased to about 1/3 power loss of traditional three supplies.

III. PRINCIPLE AND TIMING

A. Principle

In the coupled supply, the secondary side of T_1 possesses two outputs, namely, Heater_out and Ignitor_Keeper_out, among which, Heater_out is the output of heater supply, while Ignitor_Keeper_out outputs high voltage pulse for igniting, or low voltage and constant set current for keeping. As shown in Fig. 3(c), there are three windings in T_1 , with turns ratio as $N_1:N_2:N_3$. Besides, the two windings at secondary side undergo rectification-filter independently, and the rectifying circuit of Ignitor_Keeper_out is overlaid onto that of Heater_out, with these two outputs based on the same basis ground. Additionally, two switches Q_1 and Q_2 , are ON or OFF simultaneously. When Q_1 and Q_2 are ON, as shown in Fig. 4(a), the power from primary side is transferred through T_1 to secondary side to charge coupling inductor L_{c1} and L_{c2} and store energy; when Q_1 and Q_2 are OFF, as shown in Fig. 4(b), there is freewheeling in L_{c1} and L_{c2} through D_4 and D_6 , and the magnetic exciting current in primary side of T_1 flows back into the power input through D_1 and D_2 .

The theoretical operating waveforms of the coupled supply is shown in Fig. 5, with T is the switching period. Before successful

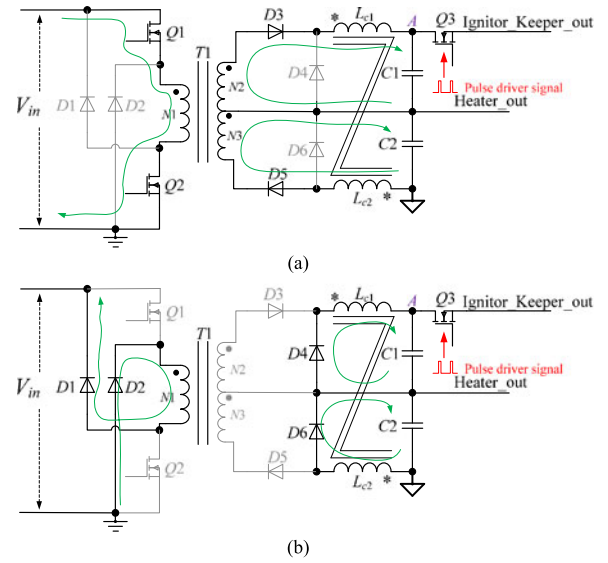


Fig. 4. Equivalent circuit diagram of heater-ignitor-keeper supply when Q_1 and Q_2 are (a) on or (b) off.

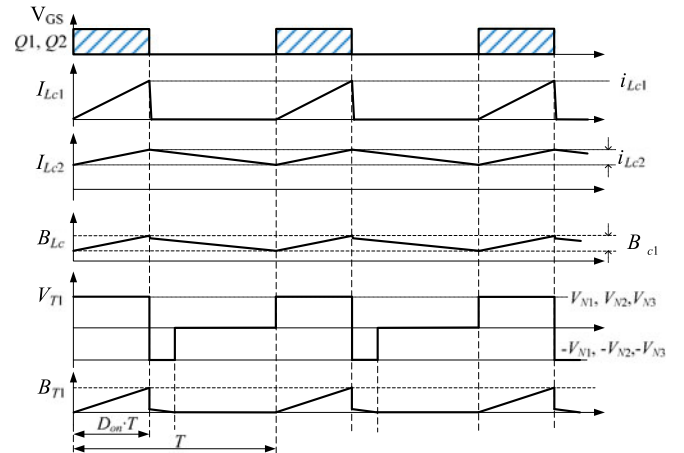


Fig. 5. Theoretical operating waveforms of the coupled supply.

ignition of hollow cathode, Heater_out outputs constant current at the set value in a settable range and provides energy to heating filament, and PWM is closed-loop controlled and regulated by heater current (I_h), and L_{c2} works at continuous current mode with peak-to-peak value of current (i_{Lc2}) determined through (1), where V_{in} is input voltage, V_{F-D5} is forward voltage of D_5 , D_{on} is duty cycle of PWM, and V_h is output voltage of Heater_out

$$i_{Lc2} = \frac{V_{in} \cdot \frac{N_3}{N_1} - V_{F-D5} - V_h}{L_{c2}} \cdot D_{on} \cdot T. \quad (1)$$

For Ignitor_Keeper_out, the high voltage pulse is generated through chopping on V_A by Q_3 . Since cathode keeper is at totally off before successful ignition, namely, the keeper impedance is high, and the output at point A is designed to provide only the power loss of dummy payload R_D (shown in Fig. 9), the output current of Ignitor_Keeper_out could not reach the limited

value of keeper current, that is, the current closed-loop of Ignitor_Keeper_out is off work. In this case, V_A depends on turns ratio of $N2:N1$ and R_D , and L_{c1} works at discontinuous current mode with peak-to-peak value of current (i_{Lc1}) determined through

$$i_{Lc1} = \frac{V_{in} \cdot \frac{N_2}{N_1} + V_h - V_A}{L_{c1}} \cdot D_{on} \cdot T. \quad (2)$$

When $Q1$ and $Q2$ are OFF, and the current through L_{c1} decreases to 0 within the time of $D'_{off} \cdot T$, the following expression (3) can be obtained:

$$\begin{cases} i_{Lc1} = \frac{V_A - V_h}{L_{c1}} \cdot D'_{off} \cdot T \\ D'_{off} < 1 - D_{on} \end{cases}. \quad (3)$$

Since L_{c1} and L_{c2} belong to the same coupling inductor L_c , the magnetic flux density of L_c (B_{Lc}) is influenced by current through L_{c1} and L_{c2} . For three windings in $T1$, each working voltage (V_{N1} , V_{N2} , V_{N3}) has three levels. When $Q1$ and $Q2$ are ON, V_{N1} , V_{N2} , and V_{N3} equal to V_{in} , $N2/N1 \cdot V_{in}$, and $N3/N1 \cdot V_{in}$, respectively; when $Q1$ and $Q2$ are OFF, and there is freewheeling of primary winding magnetic exciting current through $D1$ and $D2$, V_{N1} , V_{N2} , and V_{N3} equal to $-V_{in}$, $-N2/N1 \cdot V_{in}$, and $-N3/N1 \cdot V_{in}$, respectively; when $Q1$ and $Q2$ are OFF, and the freewheeling is finished, V_{N1} , V_{N2} , and V_{N3} all equal to 0. Thus, the magnetic core of $T1$ is in one-way magnetization, with peak value of magnetic flux density B_{T1} determined by V_{in} and on-time of $Q1$ and $Q2$ ($D_{on} \cdot T$). Since the output of Ignitor_Keeper_out at point A only provides the power loss of R_D , V_A is close to the sum of peak voltage at $N2$ and output voltage from Heater_out. In this case, L_{c2} in Heater_out still works at continuous current mode, and the output voltage of Ignitor_Keeper_out and Heater_out can be given by

$$\begin{cases} V_{Ignitor_Keeper_A} = \frac{V_{in} \cdot N_2}{N_1} + V_{Heater_out} \\ V_{Heater_out} = \left(\frac{V_{in} \cdot N_3}{N_1} - V_{F_D5} \right) \cdot D_{on} \end{cases}. \quad (4)$$

After successful ignition, the control mode of supply is changed from current closed-loop control of Heater_out to that of Ignitor_Keeper_out, and Ignitor_Keeper_out outputs constant set current I_{ik} to keep plasma state of xenon. At this time, the keeper voltage is determined by keeper impedance (R_K), which is dependent on the structure of hollow cathode, flow rate of xenon, and working state of thruster, that is, the keeper voltage changes along with the change in working condition of thruster. L_{c2} in the output of Heater_out works at continuous current mode, and the output voltage of Ignitor_Keeper_out and Heater_out can be shown in (5), where V_{Q3} is the drop voltage of $Q3$

$$\begin{cases} V_{Ignitor_Keeper_A} = I_{ik} \cdot R_K + V_{Q3} \\ V_{Heater_out} = \left(\frac{V_{in} \cdot N_3}{N_1} - V_{F_D5} \right) \cdot D_{on} \end{cases}. \quad (5)$$

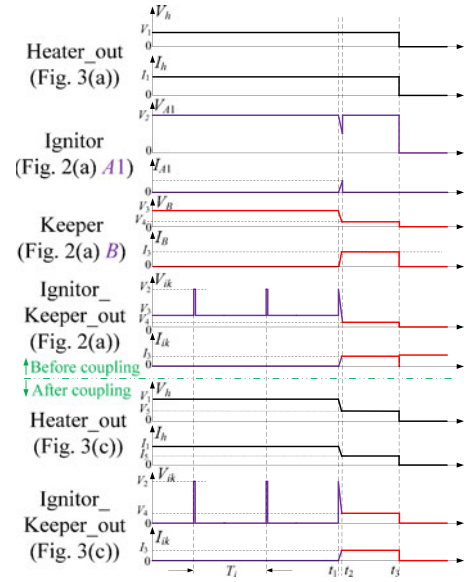


Fig. 6. Voltage/current timing waveform of each supply before coupling and after coupling during igniting process of hollow cathode in hall thruster.

B. Timing

After the coupling of traditional three supplies into heater-ignitor-keeper supply, the voltage/current waveforms of each supply before coupling and after coupling during igniting process of hollow cathode would change, as can be seen in Fig. 6.

$0 \sim t_1$: the successful ignition has not been achieved.

During this time, there is no difference between output current/voltage of Heater_out (I_h/V_h) in traditional three supplies and coupled supply, I_h is set at the value of I_1 , and V_h is V_1 , which changes with the change of heating filament resistance (R_h). For output current/voltage of Ignitor_Keeper_out (I_{ik}/V_{ik}), I_{ik} is 0 and V_{ik} is the pulse voltage with peak/valley value of $V_2/0$ in coupled supply, while I_{ik} is 0 and V_{ik} is the pulse voltage with peak/valley value of V_2/V_3 (drop voltage of $D9$ is ignored, same below) in traditional three supplies, where V_2 is the output voltage of ignitor supply (voltage at point A1 in Fig. 2(a), V_{A1}) and V_3 is the output voltage of keeper supply (voltage at point B in Fig. 2(a), V_B).

$t_1 \sim t_2$: the igniting is under progress.

During this time, the igniting process begins when the peak value of pulse voltage is coming, then V_{ik} decreases to V_4 , and I_{ik} increases to I_3 from 0 for both traditional supplies and coupled supply. Following that, for coupled supply, the control mode changes from current closed-loop control of Heater_out to current limitation closed-loop control of Ignitor_Keeper_out, $Q3$ is on all the time after identifying successful ignition, and Heater_out is under open-loop control. Since PWM duty cycle corresponding to current limitation closed-loop control of Ignitor_Keeper_out is smaller than that corresponding to current closed-loop control of Heater_out, V_h decreases to V_5 from V_1 and I_h decreases to I_5 from I_1 . For traditional three supplies, I_h keeps constant, V_{A1} decreases from V_2 , and I_{A1} increases from 0 at first, and then V_{A1} and I_{A1} (output current of ignitor supply) return to V_2 and 0, respectively, when $Q3$ is OFF after

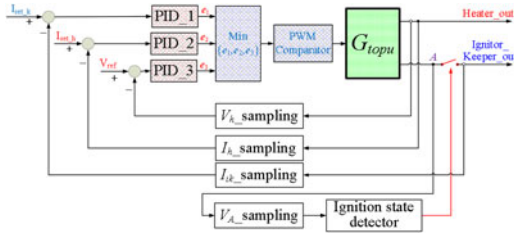


Fig. 7. Scheme of three-loop control and chopping switch logic control in the coupled supply.

identifying successful ignition; for keeper supply, V_B decreases to V_4 from V_3 , while I_B (output current of keeper supply) increases to I_3 from 0.

$t_2 \sim t_3$: the successful ignition of thruster followed the successful ignition of hollow cathode has been identified by EP control system.

During this time, for traditional three supplies, I_h still keeps constant, and there is self-heating in hollow cathode, thus, there would be great increase in the temperature of hollow cathode. The longer this process is, the shorter the useful life of hollow cathode would be. The period from t_2 to t_3 is also the response time of I_h after successful ignition, which is determined according to the identification time of EP control system on the successful ignition of hollow cathode and anode in EP thruster, the command sent time and the command execution time. This response time for the traditional three supplies is about at least 500 ms according to the engineering experience. For coupled supply, I_h is much smaller than that in traditional three supplies, thus the useful life of hollow cathode could be extended.

$t_3 \sim \rightarrow$: supplies have been shut down under the command from EP control system.

At this time, for hall thruster, both the coupled supply and all the traditional three supplies have been shut down, and the anode supply in PPU could keep plasma state of xenon. For ion thruster, in coupled supply, Heater_out stops outputting power for heating filament by closing switch between Heater_out and heater, and Ignitor_Keeper_out still outputs power to maintain plasma state of xenon; while in traditional three supplies, heater supply, and ignitor supply have been shut down, and keeper supply should be on all the time to keep plasma state of xenon.

It should be noted that the required timing of Heater_out and Ignitor_Keeper_out in the coupled supply depends completely on the design of control strategy, which is shown below.

IV. CONTROL STRATEGY

In this part, the design of three-loop control, current sampling, and chopping switch control is illustrated with details shown below.

A. Three-Loop Control

In the coupled supply, there are two outputs (Heater_out and Ignitor_Keeper_out) with three electric characteristics (heating, igniting, and keeping), which is achieved through regulation on PWM duty cycle of $Q1$ and $Q2$, and logic control on $Q3$. Fig. 7

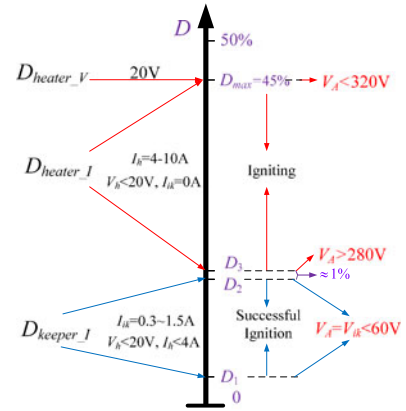


Fig. 8. Distribution of PWM duty cycle for three closed-loops.

shows the scheme of three-loop control and chopping switch logic control in the coupled supply, which also includes the sampling of voltage and current, minimizing operation on three PID outputs, etc.

As can be seen in Fig. 7, three-loop control consists of closed-loop control of I_h , clamping loop control of V_h , and limiting loop control of I_{ik} , and each output is controlled through regulation on the output error voltage signal of corresponding PID (e_1 , e_2 , e_3). With minimizing operation on e_1 , e_2 , and e_3 , the three closed-loop control provides decreasing control on the coupled supply. The minimum error voltage signal is transformed into duty cycle through PWM comparator, with duty cycle used to regulate the output of coupled supply. The three levels of duty cycle, that is the level of duty cycle when clamping loop control of V_h at work (D_{heater_V}), the level of duty cycle when closed-loop control of I_h at work (D_{heater_I}), and the level of duty cycle when limiting loop control of I_{ik} at work (D_{keeper_I}), should conform to following (6), with distribution of PWM duty cycle for three loops shown in Fig. 8

$$\begin{cases} D_{keeper_I} < D_{heater_I} < D_{heater_V} \\ D_{heater_V} = D_{max} < 45\% \\ D_3 < D_{heater_I} < D_{max} \\ D_1 < D_{keeper_I} < D_2 \\ D_3 - D_2 \approx 1\% \end{cases} \quad (6)$$

In (6) and Fig. 8, the maximum duty cycle of PWM is limited to 45% so as to ensure the effective magnetic reset of $T1$ in dual-switch forward topology. For clamping control loop of V_h , it is used to limit V_h to 20 V, which corresponds to the maximum duty cycle (D_{max}) of the supply in steady operation. In closed-loop control of I_h , the minimum D_{heater_I} (D_3) corresponds to the minimum V_h . When the duty cycle is between $[D_3, D_{max}]$, V_A is under open-loop control, with the value designed as $V_A < 320$ V at D_{max} and designed as $V_A > 280$ V at D_3 . In limiting loop control of I_{ik} , the duty cycle D_{keeper_I} is between D_1 and D_2 , which completely depends on the set value of I_{ik} and keeper impedance. Additionally, there should be an interval of about 1% between D_3 and D_2 .

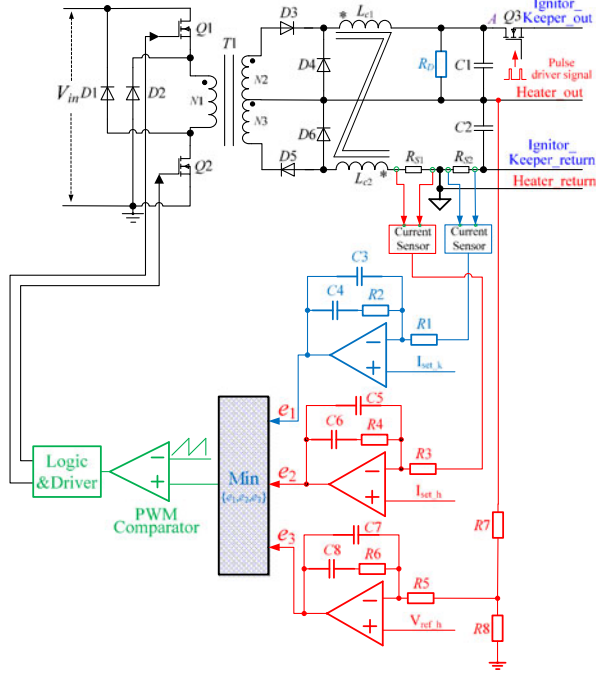


Fig. 9. Three-loop control circuit sketch of the coupled supply.

Fig. 9 shows the three-loop control circuit sketch of the coupled supply, which achieves the following functions:

1) *Closed-loop control of I_h* : During heating process, R_h changes slowly with the change of heating filament temperature, and there is high requirement for precise and stable control on I_h and low requirement for dynamic response of I_h , thus, I_h is sampled and under closed-loop control with basis reference I_{set_h} set through commands. Before successful ignition, I_h could be set between 4 and 10 A, and PWM duty cycle of the coupled supply changes in the range of $[D3, D_{max}]$. At this time, there is no closed-loop control on V_A , and V_A changes within a specified range by designing appropriate turn ratio ($N2: N1$) of $T1$ and resistance value of R_D .

2) *Clamping Loop Control of V_h* : Since R_h increases with the increase of heating filament temperature, so does V_h when I_h is set to be constant, there should be a limitation on V_h to avoid the damage of hollow cathode and the coupled supply. In this paper, V_h is limited at 20 V through closed-loop control of V_h by setting basis reference V_{set_h} at 20 V.

3) *Limiting Loop Control of I_{ik}* : At the moment of successful ignition, there is a severe dynamic regulation of V_{ik} and I_{ik} until to the achievement of stable plasma in hollow cathode. After the stable plasma is obtained, there is low level of keeper impedance, and I_{ik} is closed-loop controlled quickly to the set limited value (that is basis reference I_{set_k} set through commands), so as to avoid the damage of coupled supply and cathode keeper.

In addition, the above three loops work independently under different periods with only one loop working each time, that is, there is switch over among different loops under different working conditions, but no interaction between loops at the same time. The PID parameters of three independent loops

are designed according to the model of main-power topology, corresponding output current/voltage, and working condition of payloads. The PID parameters should ensure the stability of corresponding closed loop during the whole working process. Additionally, three loops correspond to different distribution of PWM duty cycle (D), and the duty cycle for limiting loop control of I_{ik} is smaller than that for clamping loop control of V_h and that for closed-loop control of I_h . The duty cycle is controlled through the minimum operation on outputs of three loops. At the moment of successful ignition, the coupled supply changes from working under closed-loop control of I_h (or clamping loop control of V_h) to working under limiting loop control of I_{ik} , and I_h automatically decreases instantaneously. This transient response is achieved through the quick close on loop control of I_{ik} after successful ignition, which is realized by adopting two measures: the chopping switch is set at on state after identification of successful ignition by ignitor supply through the detection of $V_{ik} < \text{set value}$ and I_{ik} is sampled through fast dynamic response and high-precision sampling circuit. The PID parameter for loop control of I_{ik} is designed to possess high bandwidth so as to ensure the fast response of I_{ik} and the quick closed loop to make I_{ik} at the set value.

B. Current Sampling

In the coupled supply, I_h is under closed-loop control before successful ignition while I_{ik} is under closed-loop control after successful ignition. For these two closed-loop control, I_h and I_{ik} should be sampled accurately, besides, the high-precise control on I_h and fast dynamic response of I_{ik} should also be ensured. Since the output filter inductor of Heater_out and that of Ignitor_Keeper_out are coupled together in the coupled supply, I_h and I_{ik} go through the same ground return. Thus, I_h and I_{ik} should be separated before being sampled, which could be obtained through specific layout of sampling resistance R_{S1} and R_{S2} , as can be seen in Fig. 9.

In Fig. 9, R_{S1} and R_{S2} are laid before filter capacitor C_2 , and are in series with L_{c2} . The Heater_return is connected between R_{S1} and R_{S2} and set as the control basis ground, while the Ignitor_Keeper_return is connected between R_{S2} and C_2 . Before successful ignition, the current through R_{S1} is just I_h , that is I_1 in Fig. 6; and R_{S2} can be considered as the equivalent ESR resistance of C_2 , then the current through R_{S2} is just the ac current ripple of C_2 (ΔI_{C2}) with its average value of 0. Thus, the control of I_h could be achieved through accurate sampling and closed-loop control of current through R_{S1} . After successful ignition, I_h and I_{ik} all flow through R_{S1} , and I_{ik} and ΔI_{C2} all flow through R_{S2} , that is, the current through R_{S1} and R_{S2} equal to $(I_5 + I_3)$ (shown in Fig. 6) and $(I_3 + \Delta I_{C2})$, respectively. Hence, the settable limitation of I_{ik} could be achieved through accurate sampling and closed-loop control of the current through R_{S2} , and filter on ΔI_{C2} . Since I_h is relatively high, the value of R_{S1} could be small, and the value of R_{S2} should be higher since I_{ik} is smaller than I_h .

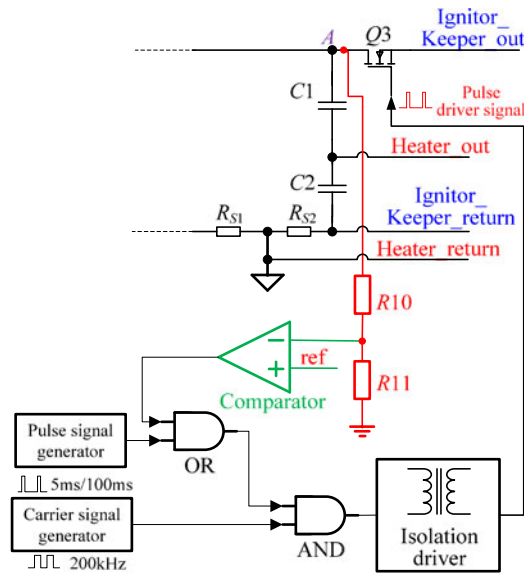


Fig. 10. Control circuit sketch of the chopping switch $Q3$.

C. Chopping Switch Control

Fig. 10 shows the control circuit sketch of $Q3$, from which it can be seen that the identification of ignition state is through sampling V_A and comparison between V_A and reference voltage by comparator. Before successful ignition, V_A is larger than designed value, and the output of comparator is “0” logic level. When V_A is identified to be lower than designed value, which is resulted from the successful ignition, the output of comparator becomes “1” logic level, and the successful ignition is identified. Then the output of comparator is under OR operation with pulse signal, which is generated in pulse signal generator and used to set the period and width of chopping switch pulse (period/width of 100 ms/5 ms are set in Fig. 10). Next, the output of OR operation is then under AND operation with carrier signal, which is generated from carrier signal generator. Thus, through control on the availability of carrier signal, the pulse carrier signal is generated, which transforms to secondary side through isolated driver transformer, and is rectified to pulse driver signal to drive $Q3$ to chop V_A , finally high voltage pulse is generated. After successful ignition, the output of OR operation is constant at “1” logic level and $Q3$ is ON all the time through continuous carrier signal.

For the novel coupling method proposed in this paper, the key idea is coupling rectification and output filter of isolated secondary side, three-loop control, sampling, and chopping switch control. It should be noted that these ideas are not limited to the application in dual-switch forward topology, that is, the coupled supply could also be obtained through the application of aforementioned key ideas in the topology of flyback, push-pull, half bridge, full-bridge, etc. The employment of dual-switch forward topology in this paper is just based on the consideration of its simple main topology, drive and control, and low voltage stress on the primary switches and secondary rectifier diodes,

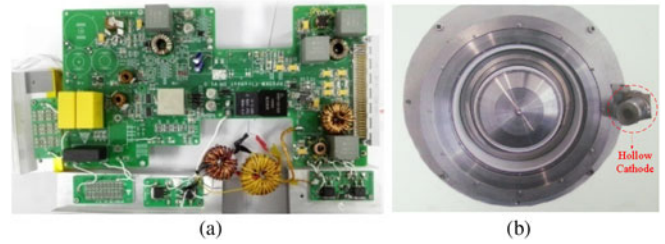


Fig. 11. (a) Heater-ignitor-keeper supply prototype and (b) photo of AEP hall thruster employed in joint test.

needless of magnetic reset. Additionally, considering the high requirement of reliability in spacecraft and the oscillation characteristic of EP thruster under the working condition, as well as the comparison with traditional three supplies, the coupled supply prototype in this paper is built through normal dual-switch forward topology without application of secondary synchronous rectification and soft switching in converter, which are two commonly used strategies to increase efficiency in industry. It should be noted that, due to the complication in designing control, transformer, and coupling inductor, the coupling of three supplies into one supply also brings disadvantage of decreased reliability, that is, any malfunction would lead to all function loss for the coupled supply. However, similar with the adoption of redundancy configuration for three traditional supplies to ensure the reliability, the reliability of coupled supply can also be ensured to adopt the redundancy configuration.

V. EXPERIMENTAL RESULTS

A heater-ignitor-keeper supply prototype, as shown in Fig. 11(a), has been built and tested, and the joint test of the coupled supply with an AEP hall thruster, which is shown in Fig. 11(b), has also been conducted. Based on the consideration that the traditional three supplies are used for powering hollow cathode of EP thruster applied in aerospace, the electronic components with the parameters corresponding to the parameters of spacecraft-grade electronic components, rather than the optimal electronic components applied in industry, are selected to build the prototype. The prototype parameters are listed in Table II. In the coupled supply, Heater_out could output current of 4–10 A and maximum voltage at 20 V, while Ignitor_Keeper_out could output pulse voltage with peak value between 280 and 320 V and pulse width/period of 5 ms/100 ms during igniting process, and output current limited at a set value between 0.3 and 1.5 A after successful ignition.

A. Electrical Characteristic Test

Before successful ignition, I_h is under closed-loop control and Ignitor_Keeper_out is at open-loop control with high voltage pulse output. By employing electronic load set at 0.68Ω as R_h , and a resistance of $1 M\Omega$ as keeper impedance of hollow cathode before successful ignition, the coupled supply is tested with voltage/current waveforms of Heater_out and Ignitor_Keeper_out shown in Fig. 12. As can be seen in Fig. 12, Heater_out outputs current (I_h) of 9 A and voltage (V_h) of

TABLE II
 PROTOTYPE PARAMETERS

Parameter	Comment	value
Switching frequency	f_s	200 kHz
Power Mosfet	Q_1, Q_2	IRFB42N20D
Pulse Chopper Mosfet	Q_3	STF20N65M5
Power Diode	D_1, D_2	STTH4R02UY
	D_3, D_4	STTH1210D
	D_5, D_6	STPS60150CT
Main Transformer	T_1	Ferroxcube TN32/19/13-3C95 $N_1 : N_2 : N_3 = 18 : 41 : 12$
Coupling Inductor	L_{c1}, L_{c2}	Magnetics, 58324 High Flux-125 $L_{c1} = 240 \mu\text{H}$ $L_{c2} = 90 \mu\text{H}$
Filter capacitor	C_1	5.6 $\mu\text{F}/600 \text{V}$
	C_2	20 $\mu\text{F}/100 \text{V}$
Dummy Resistance	R_D	50 k Ω
Sample Resistance	R_{S1}	5 m Ω
	R_{S2}	20 m Ω

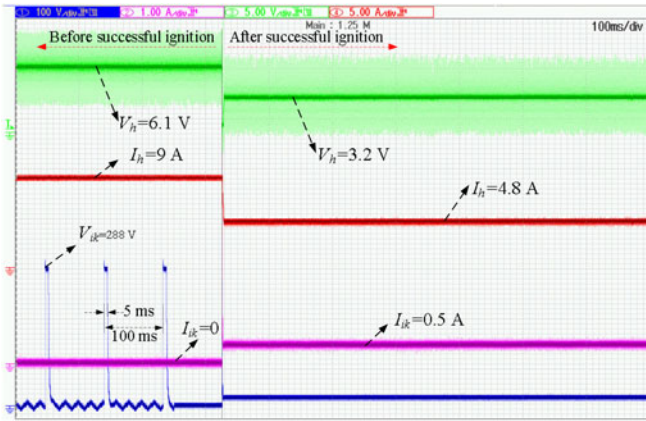
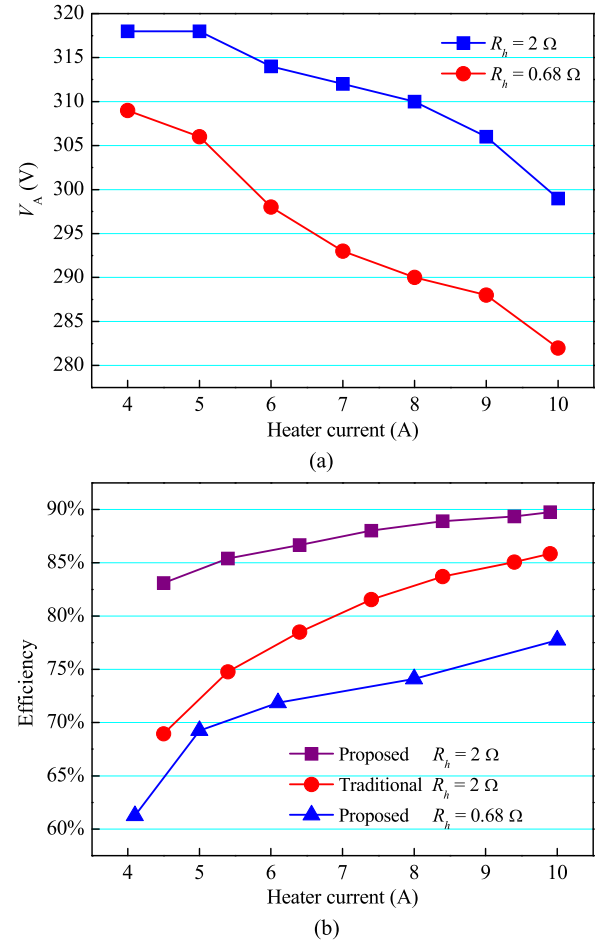


Fig. 12. Voltage/current waveforms of Heater_out and Ignitor_Keeper_out during the electrical characteristic test.

6.12 V, while Ignitor_Keeper_out outputs pulse voltage with pulse width/period of 5 ms/100 ms, and peak/valley value of 288 V/0. The peak voltage at Ignitor_Keeper_out equals to V_A .

At the moment of successful ignition, keeper impedance decreases sharply and the coupled supply is tested by adopting air switch to make Ignitor_Keeper_out short-circuit with voltage/current waveforms of Heater_out and Ignitor_Keeper_out also illustrated in Fig. 12. As can be seen in Fig. 12, at the moment of short-circuit, I_h decreases to 4.8 from 9 A, V_h decreases to 3.2 from 6.1 V, while V_{ik} decreases and I_{ik} increases to 0.5 A, achieving the purpose of quick decrease on the heating power.

Fig. 13(a) shows the change of V_A along with the change of I_h in the range of 4–10 A with R_h at 0.68 or 2 Ω , from which it can be seen that, V_A increases when I_h decreases or R_h increases (that is, V_h increases), and V_A changes between 280 and 320 V, in agreement with the design expectation. For the power loss of traditional three supplies, it is mainly from auxiliary power supply, primary side switching transistor, power transmission of isolated transformer, secondary-side rectification diode, filter capacitor, etc. The experiments show that, the power of auxiliary power supply is similar for three traditional supplies with value


 Fig. 13. (a) Plot of V_A under I_h in the range of 4–10 A and R_h at 0.68 or 2 Ω ; and (b) plot of the coupled supply efficiency under I_h in the range of 4–10 A and R_h at 0.68 or 2 Ω , and traditional three supplies efficiency under I_h in the range of 4–10 A and R_h at 2 Ω .

at 90 mA/12 V, and other power loss changes along with the change of working conditions. Fig. 13(b) shows the efficiency variation of coupled supply when I_h changes in the range of 4–10 A and R_h is 0.68 or 2 Ω , from which it can be seen that, the efficiency increases with the increase of V_h (corresponds to the increase of R_h) and I_h , and the auxiliary power supply of coupled supply increases to 120 mA, smaller than the total auxiliary power supply of traditional three supplies (270 mA). Besides, the maximum efficiency could reach to 89.7% at the V_h of 20 V (corresponds to the R_h of 2 Ω) and I_h of 10 A. Additionally, with R_h of 2 Ω and I_h in the range of 4–10 A, the efficiency of traditional three supplies has also been shown in Fig. 13(b) for comparison with coupled supply, with results demonstrating that the efficiency of coupled supply increases by 3.9–14.2% as being compared with that of traditional three supplies, and the smaller I_h is, the more the efficiency increases.

B. Joint Test of the Coupled Supply With AEP Hall Thruster

Fig. 14 shows the voltage/current waveforms of Heater_out and Ignitor_Keeper_out at the successful ignition moment of hollow cathode during the joint test of the coupled supply with

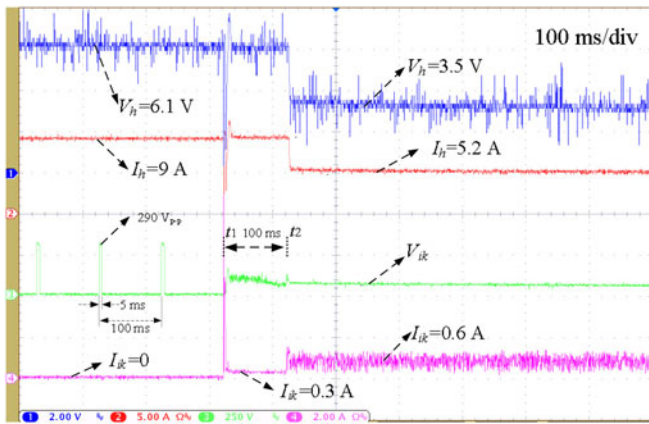


Fig. 14. Voltage/current waveforms of Heater_out and Ignitor_Keeper_out at the successful ignition moment of hollow cathode during the joint test.

AEP hall thruster. By setting I_h at 9 A, V_h is 5.2 V at first and then increases with the heating time during igniting process. At close to successful ignition, Ignitor_Keeper_out outputs current of 0 and pulse voltage with peak value of 290 V; when V_h increases to 6.1 V, the successful ignition is obtained at one pulse rise of pulse voltage (that is, at the time of t_1), and followed by successful ignition of thruster. During the time from t_1 to t_2 , the plasma at anode and hollow cathode is under severe dynamic regulation with regulation time of 100 ms in our test, and V_{ik} is clamped at 115 V at first and then decreases oscillatorily to 70 V, and I_{ik} shows a current peak at 8.9 A at t_1 and is then limited at 0.3 A. After t_2 , I_{ik} is limited at 0.6 A under closed-loop control, V_h decreases to 3.5 V sharply, I_h is under open loop control and decreases to 5.2 A within the period <0.5 ms, which is much smaller than the response time of I_h for traditional three supplies (>500 ms), achieving the purpose of sharp decrease of I_h at the moment of successful ignition, that is, the purpose of fast dynamic response.

It should be noted that, for the above employed hollow cathode, I_h is set at 9 A, and due to small R_h , V_h only increases to 6.1 V during igniting process, which is smaller than 20 V, thus clamping loop control of V_h is out of work all the time.

VI. CONCLUSION

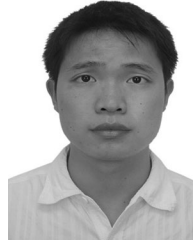
This paper presents a coupling method of power supplies to improve power density, efficiency, and dynamic response for future application in aerospace or specific industrial equipment. By taking the case of heater supply, ignitor supply, and keeper supply for hollow cathode of an AEP Hall thruster, the design, working principle, timing characteristic, and control strategy for the coupled supply obtained with the proposed coupling method were described in detail. Additionally, a coupled supply prototype was developed and tested with results showcasing the functionality of the proposed novel coupling method. That is, the power density is improved since three supplies are coupled into one supply; the coupled supply prototype shows the maximum efficiency of 89.7%, increasing by 3.9–14.2% as being compared with that of traditional three supplies with heater current between 4 and 10 A; and the joint test of the coupled

supply prototype with an AEP hall thruster shows the sharp decrease of heater current at the moment of successful ignition, thus achieving the fast dynamic response and extending useful life of hollow cathode. These results clearly demonstrate that the improvements in power density, efficiency, and dynamic response of power supply can be achieved through the application of the proposed novel coupling method.

REFERENCES

- [1] Q. Li, Y. Dong, F. C. Lee, and D. J. Gilham, "High-density low-profile coupled inductor design for integrated point-of-load converters," *IEEE Trans. Power Electron.*, vol. 28, no. 1, pp. 547–554, Jan. 2013.
- [2] B. Whitaker *et al.*, "A high-density, high-efficiency, isolated on-board vehicle battery charger utilizing silicon carbide power devices," *IEEE Trans. Power Electron.*, vol. 29, no. 5, pp. 2606–2617, May 2014.
- [3] J. Biela, U. Badstuebner, and J. W. Kolar, "Impact of power density maximization on efficiency of dc-dc converter systems," *IEEE Trans. Power Electron.*, vol. 24, no. 1, pp. 288–300, Jan. 2009.
- [4] L. Hyung-Woo, K. Tae-Hyung, and M. Ehsani, "Practical control for improving power density and efficiency of the BLDC generator," *IEEE Trans. Power Electron.*, vol. 20, no. 1, pp. 192–199, Jan. 2005.
- [5] H. Sarnago, O. Lucia, A. Mediano, and J. M. Burd, "Multi-mosfet-based series resonant inverter for improved efficiency and power density induction heating applications," *IEEE Trans. Power Electron.*, vol. 29, no. 8, pp. 4301–4312, Aug. 2014.
- [6] B. Cougo, H. Schneider, and T. Meynard, "High current ripple for power density and efficiency improvement in wide bandgap transistor-based buck converters," *IEEE Trans. Power Electron.*, vol. 30, no. 8, pp. 4489–4504, Aug. 2015.
- [7] H. Wang and F. Wang, "Power MOSFETS paralleling operation for high power high density converters," in *Proc. 41st Annu. Meeting 2006 IEEE Ind. Appl. Conf.*, 2006, vol. 5, pp. 2284–2289.
- [8] T. Das, S. Prasad, S. Dam, and P. Mandal, "A pseudo cross-coupled switch-capacitor based dc-dc boost converter for high efficiency and high power density," *IEEE Trans. Power Electron.*, vol. 29, no. 11, pp. 5961–5974, Nov. 2014.
- [9] W. Jia and F. C. Lee, "Two novel soft-switched, high frequency, high-efficiency, non-isolated voltage regulators—the phase-shift buck converter and the matrix-transformer phase-buck converter," *IEEE Trans. Power Electron.*, vol. 20, no. 2, pp. 292–299, Mar. 2005.
- [10] G. Yu, Z. Donglai, and Z. Zhongyang, "Input current ripple cancellation technique for boost converter using tapped inductor," *IEEE Trans. Ind. Electron.*, vol. 61, no. 10, pp. 5323–5333, Oct. 2014.
- [11] W. Jing, W. G. Dunford, and K. Mauch, "Analysis of a ripple-free input-current boost converter with discontinuous conduction characteristics," *IEEE Trans. Power Electron.*, vol. 12, no. 4, pp. 684–694, Jul. 1997.
- [12] Y. Dong, "Investigation of multiphase coupled-inductor buck converters in point-of-load applications," Ph.D. dissertation, Bradley Dept. Elect. Comput. Eng., Virginia Polytech. Inst. State Univ., Blacksburg, VA, USA, 2009.
- [13] S. A. Wibowo *et al.*, "Analysis of coupled inductors for low-ripple fast-response buck converter," *IEICE Trans. Fundam. Electron., Commun. Comput. Sci.*, vol. 92, no. 2, pp. 451–455, 2009.
- [14] E. Sanchis *et al.*, "Bidirectional high-efficiency nonisolated step-up battery regulator," *IEEE Trans. Aerosp. Electron. Syst.*, vol. 47, no. 3, pp. 2230–2239, Jul. 2011.
- [15] Z. Xunwei, P. Xu, and F. C. Lee, "A high power density, high efficiency and fast transient voltage regulator module with a novel current sensing and current sharing technique," in *Proc. 14th Annu. Appl. Power Electron. Conf. Expo.*, 1999, vol. 1, pp. 289–294.
- [16] Y. Zhang and D. Xu, "Design and implementation of an accurately regulated multiple output ZVS dc-dc converter," *IEEE Trans. Power Electron.*, vol. 22, no. 5, pp. 1731–1742, Sep. 2007.
- [17] H. Wu, C. Wan, K. Sun, and Y. Xing, "A high step-down multiple output converter with wide input voltage range based on quasi two-stage architecture and dual-output LLC resonant converter," *IEEE Trans. Power Electron.*, vol. 30, no. 4, pp. 1793–1796, Apr. 2015.
- [18] J. K. Kim, S. W. Choi, C. E. Kim, and G. W. Moon, "A new standby structure using multi-output full-bridge converter integrating flyback converter," *IEEE Trans. Ind. Electron.*, vol. 58, no. 10, pp. 4763–4767, Oct. 2011.

- [19] Y. Chen, Y. Kang, S. Nie, and X. Pei, "The multiple-output dc-dc converter with shared ZCS lagging leg," *IEEE Trans. Power Electron.*, vol. 26, no. 8, pp. 2278–2294, Aug. 2011.
- [20] A. Barrado, E. Olias, A. Lazaro, J. Pleite, and R. Vazquez, "PWM-PD multiple output dc/dc converters: Operation and control-loop modeling," *IEEE Trans. Power Electron.*, vol. 19, no. 1, pp. 140–149, Jan. 2004.
- [21] A. Capel and P. Perol, "Comparative performance evaluation between the s4r and the s3r regulated bus topologies," in *Proc. 2001 IEEE 32nd Annu. Power Electron. Spec. Conf.*, 2001, pp. 1963–1969.
- [22] J. E. Scina, M. Aulisio, S. S. Gerber, F. Hewitt, and L. Miller, "Power processing for a conceptual project prometheus electric propulsion system," presented at the 40th Joint Propulsion Conf. Exhib., Fort Lauderdale, FL, USA, Jul. 11–14, 2004.
- [23] H. De Clercq, C. Rijm, E. Bourguignon, T. Scalais, and V. Lempereur, "High power processing unit for stationary plasma thruster," in *Proc. 3rd Int. Spacecraft Propulsion Conf.*, Cannes, France, 2000, pp. 1–6.
- [24] O. Mourra, A. Fernandez, S. Landstroem, and F. Tonicello, "Buck-buck-boost regulator (b³r) for spacecraft power conditioning unit," presented at the 9th Eur. Space Power Conf., Saint Raphaël, France, Jun. 6–10, 2011.
- [25] H. Zhu, D. Zhang, B. Zhang, and Z. Zhou, "A non-isolated three-port dc-dc converter and three domain control method for pv-battery power systems," *IEEE Trans. Ind. Electron.*, vol. 62, no. 8, pp. 4937–4947, Aug. 2015.
- [26] Z. Tianping, Y. Le, T. Licheng, and W. Liang, "The electric propulsion progress in lip," presented at the 30th Int. Symp. Space Technology Science, 34th Int. Electric Propulsion Conf., and 6th Nano-Satellite Conf., Kobe-Hyogo, Japan, Jul. 4–10, 2015.
- [27] J. G. d. Amo, "European space agency (ESA) electric propulsion activities," presented at the 30th Int. Symp. Space Technology Science, 34th Int. Electric Propulsion Conf., and 6th Nano-Satellite Conf., Kobe-Hyogo, Japan, Jul. 4–10, 2015.
- [28] J. J. Delgado, J. A. Baldwin, and R. L. Corey, "Space systems loral electric propulsion subsystem: 10 years of on-orbit operation," presented at the 30th Int. Symp. Space Technology Science, 34th Int. Electric Propulsion Conf., and 6th Nano-Satellite Conf., Kobe-Hyogo, Japan, Jul. 4–10, 2015.
- [29] H. Osuga *et al.*, "Development status of power processing unit for 250mm-class hall thruster," presented at the Proc. 8th Eur. Space Power Conf., Constance, Germany, Sep. 14–19, 2008.
- [30] P. Stuckey, C. Clauss, M. Day, and V. Murashko, "Spt-140 high performance hall system (HPHS) development," presented at the 34th AIAA/ASME/SAE/ASEE Joint Propulsion Conf. Exhib., Cleveland, OH, USA, Jul. 10, 1998.
- [31] B. Vancil, V. Schmidt, J. Lorr, and W. Ohlinger, "Scandate hollow cathode for ion thruster," in *Proc. IEEE Int. Vac. Electron. Conf.*, Monterey, CA, USA, 2014, pp. 57–58.
- [32] L. R. Piñero, T. Bond, D. Okada, K. Phelps, and S. Wiseman, "Design of a modular 5-kw power processing unit for the next-generation 40-cm ion engine," presented at the 27th Int. Electr. Propul. Conf., Pasadena, CA, USA, Oct. 15–19, 2001.
- [33] D. J. Milligan and S. B. Gabriel, "Generation of experimental plasma parameter maps around the baffle aperture of a kaufman (uk-25) ion thruster," *Acta Astronautica*, vol. 64, no. 9–10, pp. 952–968, 2008.
- [34] Y. Oshio, K. Kubota, Y. Ohkawa, and S. Cho, "Thermal analysis of lanthanum hexaboride hollow cathode with radiative carbon heater," presented at the 30th ISTS, 34th IEPC, and 6th NSAT Conf., Kobe-Hyogo, Japan, Jul. 4–10, 2015.
- [35] D. Pedrini, R. Albertoni, F. Paganucci, and M. Andrenucci, "Modeling of lab6 hollow cathode performance and lifetime," *Acta Astronautica*, vol. 106, pp. 170–178, Jan/Feb. 2015.
- [36] Y. Ohkawa, Y. Hayakawa, H. Yoshida, K. Miyazaki, H. Nagano, and S. Kitamura, "Hollow cathode life test for the next-generation ion engine in jaxa," in *Proc. 30th Int. Elect. Propulsion Conf.*, Florence, Italy, 2007, pp. 1030–1037.
- [37] S. Ronald, P. Jeffrey, S. John, and E. Daniel, "Performance effects of interaction between a low-power arcjet and its power processing unit," presented at the 28th Joint Propulsion Conf. Exhib., Nashville, TN, USA, Jul. 6–8, 1992.
- [38] P. Delporte, P. Fayt, M. Gak, and E. Pequet, "EPC and TWTA for telecommunication satellites," in *Proc. 5th Eur. Space Power Conf.*, 1998, pp. 305–310.



Ming Fu (S'12) was born in Hubei, China, in 1984. He received the B.S. degree from Harbin Institute of Technology, Harbin, China, in 2007, and the M.S. degree from Harbin Institute of Technology Shenzhen Graduate School, Shenzhen, China, in 2009, where he is currently working toward the Ph.D. degree in power electronics and power drives.

He is also a Power Electronics Engineer in Shenzhen Academy of Aerospace Technology, Shenzhen, China.

His research interests include space power conditioning unit, electric propulsion power processing unit, and fuel battery energy system.



Donglai Zhang (M'03) was born in Jilin, China, in 1973. He received the B.S., M.S., and Ph.D. degrees from Harbin Institute of Technology, Harbin, China, in 1994, 1996, 1999, respectively.

Since 2005, he has been a Professor at Harbin Institute of Technology Shenzhen Graduate School. His research interests include analysis, modeling and control of power converters, digital control techniques for power electronic circuits, and grid-connected converters for renewable energy systems. In these research fields, he was leading several industrial and

government projects.

Prof. Zhang is a Member of the China Power Electronics Society.



Tiejai Li was born in Shanghai, China, in 1950. He received the B.S. and M.S. degrees in electrical engineering from the Harbin Institute of Technology, Harbin, China, in 1977 and 1990, respectively.

Since 1985, he has been a Member of the Faculty at the Harbin Institute of Technology. He was a Lecturer, Associated Professor, and Professor with the Department of Electrical Engineering, in 1985, 1990, and 1996, respectively. His research interests include the design and control of permanent-magnet motor and drives, design of control IC, and integrated motor

research. He was the Outstanding Contribution Expert of China Aerospace Industrial Department in 1997. Now, he is also the Chief Technical Engineer of the Shenzhen Academy of Aerospace Technology, Shenzhen, China.